

# Valence calculations of actinide anion binding energies: All bound $7p$ and $7s$ attachments

Steven M. O'Malley and Donald R. Beck

*Department of Physics, Michigan Technological University, Houghton, Michigan 49931, USA*

(Received 5 June 2009; published 16 September 2009)

Relativistic configuration-interaction calculations have been performed for anion binding energies of the entire actinide row using a corelike treatment of the  $5f$  subshell: the same occupancy and universal  $jls$  restrictions are applied to the subshell throughout the basis of each neutral and anion calculation. We predict bound  $7p$  attachments to all actinide ground state configurations except Fm, Md, and No. Additional anion bound states are formed by  $7p$  attachment to excited thresholds in Pa and Lr as well as  $7s$  attachments relative to excited open- $s$  thresholds in Th, Pa, U, and Np. Of the 41 bound actinide anion states presented, over half are characterized here for the first time. The most unusual case is Pa<sup>-</sup>, where these *ab initio* calculations predict five bound anion states arising from four different configurations.

DOI: [10.1103/PhysRevA.80.032514](https://doi.org/10.1103/PhysRevA.80.032514)

PACS number(s): 32.10.Hq, 31.15.am, 31.15.ve, 31.15.vj

## I. INTRODUCTION AND MOTIVATION

Our recent relativistic configuration-interaction (RCI) studies of lanthanide anion binding energies (BE's) [1,2] benefited greatly from our technique of creating universal  $jls$  restrictions on the  $4f$  subshell. The closer an  $f$  subshell is to half full, the more computationally complex the bases become, both in terms of the many-electron basis functions and the number of antisymmetrized determinants of one-electron basis functions that constitute them. Treating the  $4f$  subshell as corelike by omitting correlation that would have changed its occupancy and fixing the  $jls$  composition of the electrons of that subshell for every correlation configuration were necessary approximations that allowed us to tackle the complex bases near the center of the lanthanide row.

This approach is well tailored to the lanthanides and actinides and specifically most useful for anion BE calculations. For example, test calculations during our lanthanide studies [1,2] showed that correlation involving  $4f6s$  double replacements would amount to a few tens of meV with negligible differential contributions between neutral and anion energies, thus justifying their omission (and greatly reducing the basis size). One could not, however, omit similar  $ds$  correlation of  $d^k s^2$ ,  $d^{k+1} s$ , and  $d^{k+2}$  configurations in a similar transition metal calculation. The fact that our RCI BE calculations rely on direct comparison of total energies of anion states with neutral ground states or low-lying attachment thresholds means that we can optimize to at most a few levels per  $J$  of the neutral spectra. Studies of other properties of these systems, such as oscillator strength calculations or photodetachments to excited thresholds, would require less trimming of the  $f$  subshell basis to optimize a greater number of levels, limiting the power of the  $jls$ -restriction technique to reduce the overall basis sizes. With these points in mind, the next logical step in our methodology is to perform this corresponding survey of the actinide anions (the fact that as computationalists we are unhindered by radioactivity is also helpful in making this choice).

As in the lanthanide case [2] it is useful to consider the positions of the lowest thresholds of various neutral configurations as listed in Table I [3,4]. For consistency, we again use the notation that  $n$  is the occupancy of the  $5f$  subshell for

neutral configurations with two additional valence electrons, i.e.,  $5f^n 7s^2$  ground-state configurations through much of the right side of the row. On the left side of the actinide row many of the ground states are  $5f^m 6d 7s^2$ , where we define  $m \equiv n-1$ , and here we also need an additional occupation number,  $q \equiv n-2=m-1$  for the Th ground state.

Our experience with the lanthanides [1,2] suggests that we should consider possible  $7p$  attachments to neutral levels within a few tenths of an eV of each atomic ground state, and for the actinides this amounts to several likely cases: Pa  $5f 6d^2 7s^2$  ( $q=1$ ) at 245 meV, Np  $5f^5 7s^2$  ( $n=5$ ) at 351 meV, Cm  $5f^8 7s^2$  ( $n=8$ ) at 151 meV [3,4], and Lr  $5f^{14} 6d 7s^2$  ( $m=14$ ) at  $\sim 160$  meV. This last  ${}^2D_{3/2}$  threshold has not been measured experimentally, but recent calculations have predicted energies of 175 [6], 165 [7], 140 [8], and 157 meV [9] for this Lr state. Our own neutral Lr RCI calculations performed for this study place this state at 174 meV above the ground state in excellent agreement with the most recent of these other values. Placing this  ${}^2D_{3/2}$  threshold relative to the  $4f^{14} 7s^2 7p \quad {}^2P_{1/2}$  ground state is a nontrivial task that does require opening of the shallow core, e.g., including  $6p7p$  vs  $6p6d$  and  $6s7p$  vs  $6s6d$  core-valence correlation, but the BE calculations themselves include valence correlation only, consistent with the rest of this study (the anion  $7p$  attachment to this  ${}^2D_{3/2}$  level has the same  $6d$  single occupancy, so the differential contribution of the omitted core-valence correlation is expected to be small). Our calculations place this  $7p$  attachment relative to our RCI position of 174 meV, but the BE can be easily shifted by the difference between one of the other theoretical values [6–9] or some future experimental measurement if the reader prefers.

Anion states representing  $6d$  attachments relative to neutral ground states are treated by our methodology as  $7s$  attachments to excited open- $s$  thresholds, minimizing the effects of omitted core-valence correlation by ensuring the same  $6d$  occupancy in the neutral and anion states. Again, the experience of our lanthanide studies [1,2] suggests that we should consider open- $s$  attachment thresholds within  $\sim 1$  eV of each neutral ground state. From Table I these possible cases are Th ( $q=0$ ) at 690 meV, Pa (both  $m=2$  and  $q=1$ ) at 868 and 940 meV, U ( $m=3$ ) at 775 meV, and Np ( $m=4$ ) at 882 meV [3,4].

TABLE I. Survey of attachment (and photodetachment) thresholds of neutral actinide atoms with the energy of the lowest level of each configuration given in eV [3–5]. The notation “g.s.” indicates the ground state configuration, and “n.a.” indicates states that are not applicable:  $n > 14$  (Lr) or  $q < 0$  (Ac). Values presented with two significant figures are semi-empirical estimates [3], and the Lr [6–9] and No [10,11] values are averages from recent computational studies.

Atom ( $n m q$ )	$5f^n7s^2$	$5f^n6d7s^2$	$5f^n6d^27s^2$	$5f^n6d7s$	$5f^n7s7p$	$5f^n6d^27s$	$5f^n7s^27p$	$5f^n6d7s7p$	$5f^n6d^37s$	$5f^n6d7s^27p$	$5f^n6d^27s7p$
Ac (1 0 -)	3.7	g.s.	n.a.	5.2	5.3	1.143	1.2	1.700	n.a.	n.a.	n.a.
Th (2 1 0)	3.409	0.966	g.s.	4.8	5.2	1.937	2.285	2.740	0.690	1.337	1.793
Pa (3 2 1)	1.614	g.s.	0.245	1.822	3.2	0.868	1.419	1.785	0.940	1.764	1.867
U (4 3 2)	0.870	g.s.	1.426	1.840	2.826	0.775	1.440	1.816	1.9	3.0	3.1
Np (5 4 3)	0.351	g.s.	2.486	1.659	2.313	0.882	1.480	1.778	3.0	3.8	4.2
Pu (6 5 4)	g.s.	0.783	4.470	1.677	1.916	1.849	2.219	2.582	5.3	5.8	6.3
Am (7 6 5)	g.s.	1.325	6.9	1.799	1.935	2.544	2.873	3.208			
Cm (8 7 6)	0.151	g.s.		2.099	2.189	1.258	1.149	1.944			
Bk (9 8 7)	g.s.	1.133		2.130	2.097	2.756	2.204	3.057			
Cf (10 9 8)	g.s.	2.097		2.543	2.165	3.9	3.066	4.210			
Es (11 10 9)	g.s.	2.401		2.9	2.207	4.5	2.7	4.5			
Fm (12 11 10)	g.s.	2.5		3.2	3.112	4.8	2.6	4.6			
Md (13 12 11)	g.s.										
No (14 13 12)	g.s.			3.513	2.341						
Lr (- 14 13)	n.a.	0.159		n.a.	n.a.			g.s.			

Of course, the remainder of the lowest-lying thresholds tabulated in Table I are much too high in the spectra to be reasonable attachment candidates, but it is useful to collect the data for those configurations that represent likely photodetachment thresholds that could be seen by experimenters. For example, the Th<sup>-</sup>  $6d^27s^27p$  ( $q=0$ ) anion states would detach via  $7p \rightarrow \epsilon s + \epsilon d$  back to the neutral  $6d^27s^2$  ground state, but additional features representing detachment to  $6d7s^27p$  via  $6d \rightarrow \epsilon p + \epsilon f$  and  $6d^27s7p$  via  $7s \rightarrow \epsilon p$  would likely also be seen for incident photon energies above  $\sim 1.5$  eV.

## II. RCI BASIS CONSTRUCTION

The RCI methodology and  $jls$ -restriction technique have been described in detail elsewhere [1,2,12]. Briefly, the  $5f$  electrons'  $jls$  composition is determined from neutral actinide calculations with a moderate level of correlation. Our RCI method is fully relativistic, but approximate total  $LS$  basis functions or  $ls$  rotation within groups of electrons are created by treating the major components of the one-electron wave functions as nonrelativistic spinors and directly diagonalizing the  $L^2+S^2$  (or  $l^2+s^2$ ) matrix. The low-lying thresholds of interest are usually quite pure ( $>90\%$ ) with regard to the  $5f^{n,m,q}$  dominant term, i.e., that with the highest  $s$  and highest  $l$  with that  $s$  as expected by Hund's rules. For this actinide study, wherever possible we retain additional terms such that a few tenths of a percent of the composition or less is discarded from our levels of interest (the manifold of the neutral ground states and the potential attachment thresholds discussed in Sec. I). Once the selection of retained terms is made, an auxiliary code [12] prepares our RCI input data by “pasting” this  $f$  subshell basis together with that of all the desired correlation configurations of the remaining valence electrons using angular momentum addition (employing the

step-down operator, 3- $j$  symbols, and the sum over  $m_j$  and  $m'_j$  that make the desired total  $J$  [12]).

Let us consider a specific example of basis set selection to illustrate the process. Figure 1 shows a comparison of the bottom five levels of neutral Np  $J=11/2$  between the experimental positions [3,4] and four different RCI bases. Also shown are two Np<sup>-</sup>  $J=6$  anion states: a  $7p$  attachment to the  $5f^46d7s^2$  ground state and a  $7s$  attachment to the  $5f^46d^27s$  second excited state of  $J=11/2$ . Because our RCI code is currently limited to 20 000 total basis functions, the correlation included in these test calculations is limited by the largest anion bases (retaining the entire  $5f^4$  basis), and both anion states are unbound relative to the neutral ground state at this stage. Note the stability of the positions of the anion states and neutral attachment thresholds despite the large shifts in the other neutral levels whose  $5f^4$  compositions were not considered in the basis selection.

The recipe used to create these bases is a bit more meticulous here than as described in the lanthanide study [2]. There we used a general rule of retaining all  $j$ 's of the dominant term as well as terms with  $s$  one less than the dominant term and  $\Delta l=0, \pm 1$ , while terms selected here are based purely on contributions to the levels of interest (the level composition was examined in greater detail). This occasionally results in retaining a small term or two that fall outside this rule, but the basis is also reduced somewhat by exclusion of some  $j$ 's of these  $ls$  terms that have little contribution to the levels of interest. Note that the same selections that optimize the two attachment thresholds shown in Fig. 1 also optimize the low-lying  $5f^46d7s^2$   $J=9/2, 7/2, 13/2$  thresholds at 252, 428, and 434 meV, respectively, as well as the  $5f^46d^27s$   $J=13/2$  level “on the other side of” this  $J=6$   $7s$  attachment.

Basis A is a complete basis that simply rotates the RCI  $jj$  basis functions to an  $ls$  basis in order to determine the largest

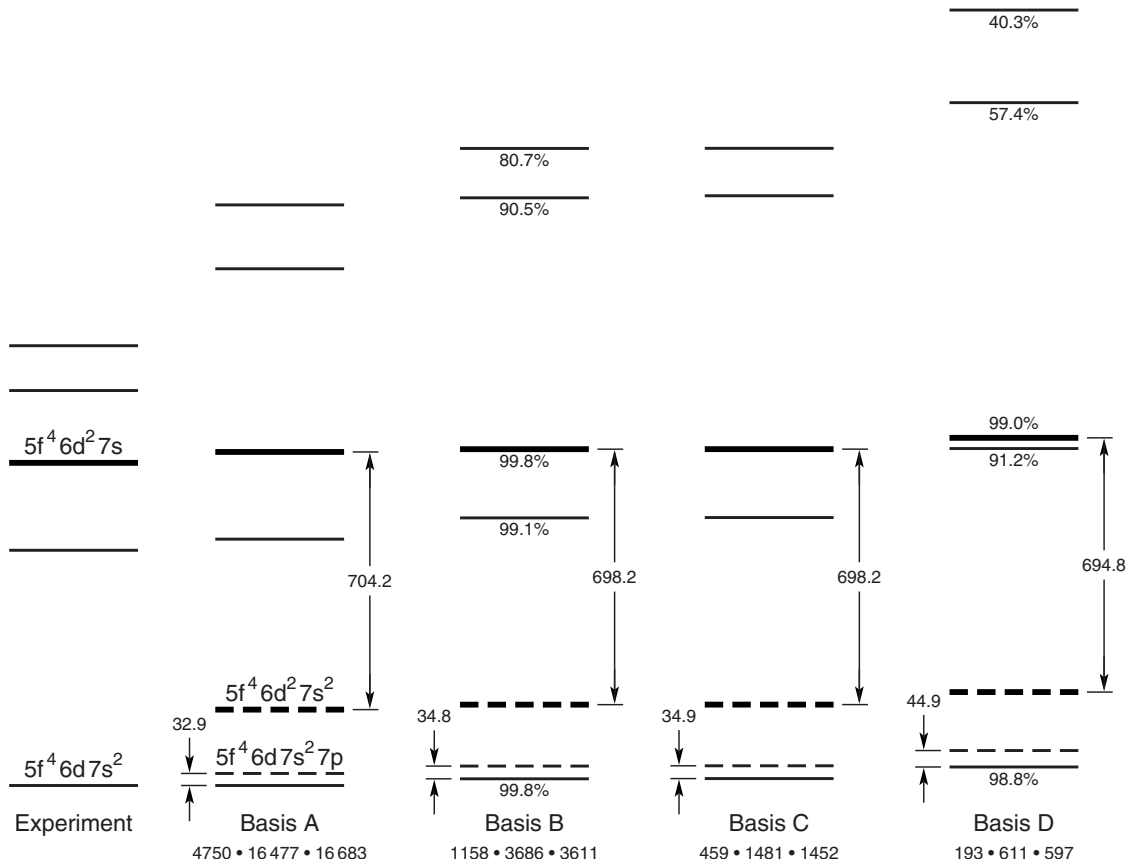


FIG. 1. An example of basis selection:  $m=4$  configurations in Np  $J=11/2$  and Np<sup>-</sup>  $J=6$ . The positions of the neutral and anion levels are shown for the four bases discussed in the text. Relative bindings of the anion states are given in meV. RCI full configuration basis sizes for the neutral, 7p attachment, and 7s attachment (thick lines) are given by the trio of numbers at the bottom of each column. The percentages in the “B” and “D” columns indicate the fraction of the  $5f^4$  basis that has been retained for each neutral level for those basis selections. The correlation configurations included in these neutral calculations are  $5f^4(6d+7s)^3$  and  $5f^4(6d+7s)7p^2$ , the 7p attachment contains  $5f^4(6d+7s)^3 7p$  and  $5f^4(6d+7s)7p^3$ , and the 7s attachment contains  $5f^4(6d+7s)^4$ ,  $5f^4(6d+7s)^2 7p^2$ , and  $5f^4 7p^4$  (additional correlation in the final calculations results in the BE’s presented in Tables II and III).

contributors to our attachment thresholds. Basis B is an intermediate stage used to determine the relative weights within each term for those with multiplicity greater than one. In a system with a  $5f^m 7s^2$  ground state, the  $5f^m ls$  composition could be taken from the total  $LS$  of the neutral calculation, but the presence of the 6d electron in the Np case means that the various  $5f^m$  ( $m=4$ )  $jls$  terms appear in calculations with different total  $J$ ’s, often with slightly different relative mixing. However, we find that relative weights within the basis functions of a given  $jls$  term are more consistent than between different  $jls$  terms, which leads us to the next step. Basis C is the primary version used in these actinide calculations, and it is produced by rotating the  $jls$  terms of Basis B with multiplicity greater than one each to a single function. In principle, Basis B could be skipped (with this composition taken directly from Basis A), but it has been included here to illustrate the negligible impact on all energy levels due to this intraterm rotation. Basis D is even further restricted and is used only in the final stages of our calculations for which our RCI bases are too complex for our coded limits (currently our RAM allows for 20 000 RCI basis functions composed of  $4 \times 10^6$  determinants and  $125 \times 10^6$  determinantal coefficients). This basis is used to determine the

differential contribution to BE’s from small but complex second-order effects or saturation of the one-electron basis sets that contribute a few tens of meV to the final energies.

For this Np example the  $jls$  terms of these bases are as follows (multiplicities greater than one given in parentheses):

$$A: {}^5I_{4,5,6,7,8}, {}^5G_{2,3,4,5,6}, {}^5F_{1,2,3,4,5}, {}^5D_{0,1,2,3,4}, {}^5S_2, {}^3M_{8,9,10}, {}^3L_{7,8,9}, {}^3K_{6,7,8}(2), {}^3I_{5,6,7}(2), {}^3H_{4,5,6}(4), {}^5G_{3,4,5}(3), {}^3F_{2,3,4}(4), {}^3D_{1,2,3}(2), {}^3P_{0,1,2}(3), {}^1N_{10}, {}^1L_8(2), {}^1K_7, {}^1I_6(3), {}^1H_5(2), {}^1G_4(4), {}^1F_3, {}^1D_2(4), {}^1S_0(2), 107 members of the complete  $5f^4$  basis.$$

$$B: {}^5I_{4,5,6}, {}^3H_{4,5}(4), {}^3G_4(3), {}^1G_4(4), 18 members kept.$$

$$C: {}^5I_{4,5,6}, {}^3H_{4,5}(1), {}^3G_4(1), {}^1G_4(1), seven members kept.$$

$$D: {}^5I_{4,5}, {}^3H_4(1), three members kept.$$

Note that not every relativistic configuration will contain all the  $jls$  terms of the full basis, e.g.,  ${}^1N_{10}$  is only present in this neutral  $J=11/2$  calculation when the remaining three-electron valence portion of the configuration can make  $j \geq 9/2$ . Nonetheless, the selection of dominant terms that retain 99.8% of the  $jls$  composition of these Np attachment thresholds results in a reduction of the basis sizes by an order

of magnitude with modest impact on the BE's (as seen in Fig. 1, the  $7p$  and  $7s$  attachments in these test calculations lost 2.0 and 6.0 meV binding, respectively, between the A and C bases). This savings is even greater for actinides closer to the center of the row, and these RCI BE calculations would not be possible without this technique.

We should point out that we have been perhaps too pessimistic in our earlier estimates [1,2] of run times for hypothetical RCI calculations that would not implement these universal  $jl$ s restrictions. While it is true that some of the most complex cases could take months of CPU time when run using an RCI bases equivalent to the complete A basis described above, it would be foolish not to perform such a calculation using the original  $jj$  basis functions. Because our RCI Hamiltonian consists of one- and two-particle operators, pairs of basis functions must differ by two or fewer electrons to produce nonzero matrix elements. Rotation to an  $ls$  basis within the  $5f^{n,m,q}$  subshell effectively removes the  $5f_{5/2}$  and  $5f_{7/2}$  occupancy present in the  $jj$  basis from consideration when comparing basis function pairs, resulting in a much less sparse energy matrix. In fact, for the test cases presented in Fig. 1, run times for the B bases were  $>20$  times faster than the A bases ( $ls$  functions) but less than 10% faster than comparable calculations using complete  $jj$  bases, i.e., the savings due to the reduction in basis size is nearly countered by the relative increase in nonzero matrix elements at that stage. However, the further rotation and reduction of basis size to the C basis that is used for the majority of our RCI calculations does produce an additional order of magnitude savings in run time in these test cases. Given these considerations, we still estimate that a hypothetical project with the computing power to perform RCI calculations without the approximations made here would require many years rather than the eight months of operator time taken to perform this actinide study.

### III. RESULTS

RCI BE's for actinide anion  $7p$  attachments are presented in Table II with total  $LS$  composition of the states taken from within the listed dominant configuration. The additional  $jj$  analysis indicates the  $j$  of the neutral core and the  $7p_{1/2}$ , " $(j)$ ," or  $7p_{3/2}$ , " $\{j\}$ ," attached electron. This latter analysis is particularly useful where cases with relative purity can predict expected features in experimental spectra, e.g., the  ${}^3F_2$  ground state of  $\text{Ac}^-$  is an attachment to the neutral  $J=3/2$  ground state (94% pure), so  $7p \rightarrow \epsilon s + \epsilon d$  photodetachment channels from this anion state that leave the atom in the  $J=5/2$  first excited state are likely to have relatively small partial cross sections. Two of our four excited configuration candidates, Pa and Lr, were found to have  $7p$  attachments with relative binding sufficient to predict bound states relative to the neutral ground states. Note that there is some ambiguity in the labeling of the  $\text{Lr}^- 5f^{14}7s^27p_{1/2}7p_{3/2}$  state, but the fact that the recent calculations [6,7,9] place the  ${}^2P_{3/2}$  level  $>1$  eV above the  ${}^2P_{1/2}$  Lr ground state, the " $\{1/2\}$ " label is the more appropriate description of the state.

The reduced density of states in the actinides [3,4] compared to analogous lanthanides [13,14] is also reflected in

anion states. For example, both Sm and Pu have  $f^6s^2 {}^7F_0$  ground states, but the first four excited states of Sm,  ${}^3F_1$  increasing in energy through  ${}^3F_4$ , lie within 282 meV of the ground state while the Pu  ${}^3F_1$  first excited state itself lies 273 meV above its ground state. Additionally, for  $4f^n6s^2$  lanthanide neutral thresholds with  $J=J_n$ , we generally saw two  $6p_{1/2}$  attachments with  $J=J_n \pm 1/2$  with similar binding and four  $6p_{3/2}$  attachments with  $J_n - 3/2 \leq J \leq J_n + 3/2$  about 100 meV above them [1], but we found this difference between  $7p_{1/2}$  and  $7p_{3/2}$  attachments in the actinides to be 175–200 meV, resulting in no bound  $7p_{3/2}$  attachments in the  $5f^n7s^2$  ground-state cases. These two points result in just one bound  $\text{Pu}^-$  anion state compared to the eight predicted  $\text{Sm}^-$  levels [1]. Another good comparison is Gd and Cm with  $f^7ds^2 {}^9D_2$  ground states. Though the first few excited  ${}^9D$  states have much closer energies than the Sm/Pu example, the  $f^7ds^2 {}^7D$  manifold lies nearly a quarter of an eV higher in Cm [3,4] than in Gd [13,14]. Comparing our predicted anion states, the  $\text{Cm}^- {}^{10}F$  manifold in Table II is actually more bound than the corresponding manifold in  $\text{Gd}^-$  [2], however, the second  ${}^8D$  manifold seen in  $\text{Gd}^-$  is much higher and unbound by about two tenths of an eV in  $\text{Cm}^-$  (this is not to say that these  ${}^8D$  manifolds are attachments to the  ${}^7D$  neutral thresholds, but simply that there is a similar increase in separation between neutral and anion manifolds in the actinide case).

Another comparison between the lanthanides and actinides is the near linearity of the  $p$  binding to  $f^n s^2$  states, including our unbound  $7p$  attachments to the excited state candidates in Np and Cm, as presented in Fig. 2. As in the lanthanide study [1], we expect that experimental measurement of the electron affinities (EAs) of any two of the actinides with  $5f^n7s^2$  ground states could be used to scale these predictions for the remaining three cases.

Actinide anion states representing  $7s$  attachments to excited open- $s$  thresholds are presented in Table III. In addition to BE's relative to the neutral ground state, we also present binding relative to the open- $s$  threshold "on either side of" each anion state's  $J$ , these being likely transition energies that may be seen by experimenters. Note that as in the case of the lanthanide  $6s$  attachments (except for  $\text{Gd}^-$  [2]), the  $LS$  terms of these neutral open- $s$  manifolds have  $L > S$ , resulting in a range of neutral thresholds with  $L - S \leq J \leq L + S$ . Because the additional  $7s$  electron closes the  $7s^2$  subshell, the corresponding anion states have the same  $L$  and an  $S$  that is  $1/2$  less than in the neutral, resulting in one fewer state in their manifold and a lack of one-to-one correspondence between attachment thresholds and potential anion bound states. Since we cannot simply "break" the  $7s^2$  subshell of the anion states to perform a  $jj$  attachment analysis similar to that of Table II, we instead present the composition of the  $(n+1)$ -electron group (excluding the single  $7s$  electron) of the neutral thresholds. The  $j$  of this group indicates the mixing of anion  $J$ 's that are created when the  $7s$  electron closes this valence subshell. The  $7s$  attachment to the lowest neutral  $J$  in each case can result only in an anion state with total  $J$  that is  $1/2$  greater (a small amount of mixing of other  $LS$  terms that can make lower neutral  $J$ 's is present in the Pa cases), while the next few attachment thresholds contain a mixture of  $j=J-1/2$  and  $j=J+1/2$ . In general, we would then expect that the photodetachment partial cross section

TABLE II. Actinide anion  $7p$  attachments with BE's given in meV and states grouped by total  $J$  (indicated in the leading  $LS$  term). The notations of the core  $j$  in the  $jj$  analysis,  $(j)$  and  $\{j\}$ , indicate  $7p_{1/2}$  and  $7p_{3/2}$  attachments, respectively. Composition in both cases is presented rounded to the nearest percent. Values in parentheses in the "BE" column indicate binding relative to the lowest threshold in cases of attachments to excited neutral configurations. The second  $7p_{1/2}$  attachment in  $\text{Es}^-$ ,  $^3K_8$ , is predicted by these *ab initio* RCI calculations to be unbound by 8 meV.

Anion total $LS$ composition	Neutral core+ $7p$ $jj$ attachment analysis	BE
$\text{Ac}^- 6d7s^27p$ ( $m=0$ )	$\text{Ac } 6d7s^2$	
$^3D_1$ 93, $^3P$ 4, $^1P$ 3	(3/2) 75, {3/2} 17, {5/2} 8	137
$^3F_2$ 52, $^1D$ 45, $^3P$ 2, $^3D$ 1	(3/2) 93, {5/2} 4, (5/2) 2, {3/2} 1	491
$^1D_2$ 47, $^3F$ 44, $^3P$ 7, $^3D$ 2	(5/2) 41, {3/2} 32, {5/2} 21, (3/2) 6	221
$^3D_2$ 89, $^3P$ 6, $^3F$ 4, $^1D$ 1	{3/2} 56, (5/2) 44	22
$^3F_3$ 96, $^3D$ 4	(5/2) 60, {3/2} 40	195
$\text{Th}^- 6d^27s^27p$ ( $q=0$ )	$\text{Th } 6d^27s^2$	
$^2S_{1/2}$ 69, $^4P$ 16, $^2P$ 8, $^4D$ 7	(0) 43, (1) 31, {2} 25, {1} 1	95
$^4F_{3/2}$ 53, $^2D$ 37, $^4D$ 8, $^2P$ 2	(2) 88, {2} 4, {0} 3, {1} 3, (1) 2	95
$^2D_{3/2}$ 54, $^4F$ 21, $^4D$ 20, $^4P$ 3, $^2P$ 2	(2) 34, {2} 29, (1) 23, {3} 12, {1} 2	19
$^4G_{5/2}$ 57, $^2F$ 32, $^2D$ 8, $^4D$ 2, $^4F$ 1	(2) 99, {4} 1	368
$^2D_{5/2}$ 41, $^4G$ 31, $^4D$ 10, $^2F$ 9, $^4F$ 6, $^4P$ 3	(2) 44, (3) 39, {2} 14, {4} 2, {3} 1	46
$^4G_{7/2}$ 82, $^2F$ 12, $^4F$ 5, $^2G$ 1	(3) 76, {2} 21, (4) 3	50
$\text{Pa}^- 5f^26d7s^27p$ ( $m=2$ )	$\text{Pa } 5f^26d7s^2$	
$^5K_5$ 59, $^3I$ 32, $^5I$ 4, $^1H$ 3, $^3H$ 2	(11/2) 67, (9/2) 24, {11/2} 9	69
$^5L_6$ 49, $^3K$ 43, $^1I$ 4, $^3I$ 2, $^5K$ 2	(11/2) 99, {11/2} 1	384
$\text{Pa}^- 5f6d^27s^27p$ ( $q=1$ )	$\text{Pa } 5f6d^27s^2$	
$^5I_4$ 50, $^3H$ 37, $^1G$ 5, $^3G$ 5, $^5H$ 2, $^3F$ 1	(7/2) 94, (9/2) 4, {9/2} 1, {7/2} 1	62 (307)
$\text{U}^- 5f^36d7s^27p$ ( $m=3$ )	$\text{U } 5f^36d7s^2$	
$^6L_{11/2}$ 50, $^4K$ 40, $^2I$ 5, $^6K$ 2, $^4I$ 2, $^2H$ 1	(5) 67, (6) 32, {6} 1	191
$^6M_{13/2}$ 56, $^4L$ 37, $^2K$ 4, $^4K$ 2, $^6L$ 1	(6) 99, {5} 1	373
$\text{Np}^- 5f^46d7s^27p$ ( $m=4$ )	$\text{Np } 5f^46d7s^2$	
$^7L_5$ 46, $^5K$ 43, $^3I$ 5, $^7K$ 3, $^5I$ 2, $^3H$ 1	(11/2) 66, (9/2) 32, {11/2} 1, {7/2} 1	86
$^7M_6$ 62, $^5L$ 32, $^3K$ 4, $^5K$ 1, $^7L$ 1	(11/2) 99, {11/2} 1	313
$\text{Pu}^- 5f^67s^27p$ ( $n=6$ )	$\text{Pu } 5f^67s^2$	
$^8G_{1/2}$ 37, $^6F$ 24, $^6D$ 18, $^8F$ 8, $^4D$ 7, $^4P$ 5, $^2P$ 1	(0) 99, {2} 1	85
$\text{Am}^- 5f^77s^27p$ ( $n=7$ )	$\text{Am } 5f^77s^2$	
$^9P_3$ 72, $^7P$ 21, $^7S$ 3, $^5P$ 2, $^7D$ 1, $^5D$ 1	(7/2) 100	76
$^9P_4$ 46, $^7P$ 46, $^5D$ 5, $^7D$ 3	(7/2) 99, {7/2} 1	53
$\text{Cm}^- 5f^76d7s^27p$ ( $m=7$ )	$\text{Cm } 5f^76d7s^2$	
$^{10}F_{3/2}$ 65, $^8D$ 28, $^8F$ 4, $^6P$ 2, $^6D$ 1	(2) 100	321
$^{10}F_{5/2}$ 60, $^8D$ 26, $^8F$ 8, $^6D$ 2, $^6P$ 2, $^6F$ 1, $^8P$ 1	(3) 56, (2) 43, {2} 1	278
$^{10}F_{7/2}$ 54, $^8D$ 25, $^8F$ 13, $^6D$ 2, $^6F$ 2, $^8G$ 1, $^6P$ 1, $^{10}D$ 1, $^8P$ 1	(3) 70, (4) 28, {3} 1, {5} 1	217
$^{10}F_{9/2}$ 46, $^8D$ 24, $^8F$ 17, $^6F$ 4, $^6D$ 2, $^8G$ 2, $^{10}D$ 2, $^{10}P$ 1, $^6G$ 1, $^8P$ 1	(4) 88, (5) 8, {4} 1, {3} 1, {5} 1, {6} 1	135
$^{10}F_{11/2}$ 35, $^8D$ 28, $^8F$ 18, $^6F$ 7, $^{10}P$ 4, $^8G$ 3, $^{10}D$ 2, $^6G$ 2, $^4G$ 1	(5) 92, {4} 3, {5} 2, {6} 2, (6) 1	13

TABLE II. (Continued.)

Anion total $LS$ composition	Neutral core+ $7p$ $jj$ attachment analysis	BE
Bk <sup>-</sup> $5f^9 7s^2 7p$ ( $n=9$ )	Bk $5f^9 7s^2$	
$^7G_7$ 42, $^5H$ 31, $^7H$ 14, $^3I$ 6, $^5I$ 5, $^3K$ 1, $^7I$ 1	(15/2) 100	31
$^5I_8$ 43, $^7H$ 30, $^7I$ 13, $^3K$ 8, $^5K$ 4, $^3L$ 1, $^1L$ 1	(15/2) 99, {15/2} 1	28
Cf <sup>-</sup> $5f^{10} 7s^2 7p$ ( $n=10$ )	Cf $5f^{10} 7s^2$	
$^6H_{15/2}$ 49, $^4I$ 30, $^6I$ 12, $^2K$ 4, $^4K$ 4, $^6K$ 1	(8) 100	18
$^4K_{17/2}$ 46, $^6I$ 26, $^6K$ 14, $^2L$ 8, $^4L$ 5, $^2M$ 1	(8) 100	10
Es <sup>-</sup> $5f^{11} 7s^2 7p$ ( $n=11$ )	Es $5f^{11} 7s^2$	
$^5H_7$ 60, $^3I$ 23, $^5I$ 14, $^3K$ 2, $^1K$ 1	(15/2) 100	2
Lr <sup>-</sup> $5f^{14} 7s^2 7p^2$ ( $m=14$ )	Lr $5f^{14} 7s^2 7p$	
$^3P_0$ 83, $^1S$ 17	(1/2) 96, {3/2} 4	465
$^3P_1$ 100	{1/2} ≡ (3/2) 100	51
Lr <sup>-</sup> $5f^{14} 6d 7s^2 7p$ ( $m=14$ )	Lr $5f^{14} 6d 7s^2$	
$^3F_2$ 65, $^1D$ 32, $^3P$ 2, $^3D$ 1	(3/2) 98, {5/2} 1, (5/2) 1	295 (469)

from the lowest anion state of each of these cases to the attachment threshold on the smaller  $J$  side to be roughly twice as large as that of the channel to the higher  $J$  side (cf. the recently predicted Pr<sup>-</sup>  $4f^2 5d^2 6s^2$  state [2] and the photoelectron kinetic energy spectrum of Davis and Thompson [15]).

Note again the presence in Table III of bound anion states for both  $m=2$  and  $q=1$  configurations of Pa<sup>-</sup>, as in the  $7p$  attachments of Table II. This suggests an incredibly interesting spectrum for Pa<sup>-</sup> since we are predicting five bound

states from four different configurations. To complicate matters, the spread of the lowest three Pa<sup>-</sup> BE's is less than 20 meV, within our expected accuracy, so the ordering of these levels is not well established.

Another observation from Table III is the consistency of the  $7s$  binding relative to the open- $s$  thresholds, averaging  $\sim 990$  meV compared to a similarly consistent  $6s$  binding of  $\sim 860$  meV in the lanthanides [2]. Finally, we note that the positions of the actinide open- $s$  attachment thresholds in the neutral spectra result in weakly bound states, such that for all actinide anions with bound states their ground state is strictly a  $7p$  attachment to the neutral ground state, unlike the lanthanide La<sup>-</sup> [2,16,17] and Ce<sup>-</sup> [2,18–20] cases.

#### IV. COMPARISONS WITH OLDER WORK

Prior to the early 1990s, calculations of actinide BE's tended to focus on  $5f$  attachments, though in at least one case a local-spin-density-functional calculation predicted a  $7p$  attachment to Am  $5f^7 7s^2$  with an EA of 103 meV [21] in reasonable agreement with our 76 meV value from Table II.

Older density-functional calculations predicted an Ac<sup>-</sup> EA of 270–410 meV [16] compared to our 491 meV, but a more recent relativistic coupled-cluster calculation resulted in an EA of 345 meV [22]. Both of these earlier calculations gave a leading  $LS$  term of  $^1D_2$ , but our RCI calculations predict greater mixing of  $^3F_2$  in the anion ground state.

Relativistic Fock-space coupled-cluster calculations predicted the same two bound Lr<sup>-</sup> configurations with bindings of 310 and 160 meV [9] compared to our 465 and 295 meV. Increased binding of anion states with time is not unprecedented or unexpected from our point of view, since (at least with the RCI methodology) passage of time leads to increased computing power and allows for additional correla-

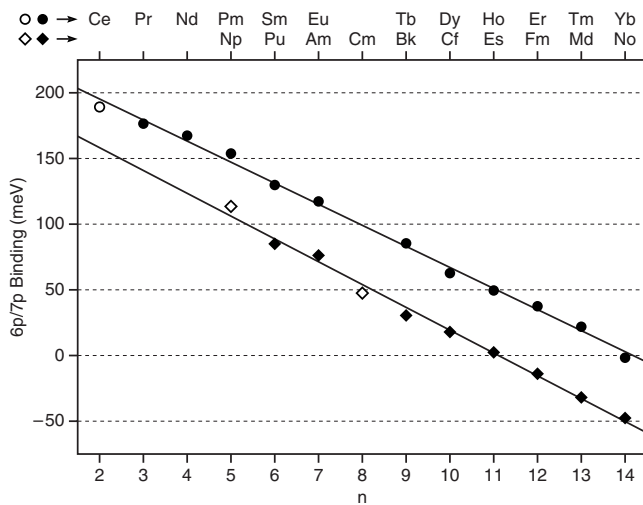


FIG. 2. Linearity of  $6p$  binding to  $4f^n 6s^2$  lanthanide states and  $7p$  binding to  $5f^n 7s^2$  actinide states. The open symbols represent the largest binding relative to excited configurations, while the full symbols are the anions' true EAs (except perhaps for Tb<sup>-</sup> where we predict that a  $6p$  attachment to the  $m=8$ , rather than  $n=9$ , configuration may be the ground state [2]).

TABLE III. Actinide anion  $7s$  attachments with BE's given in meV and total  $J=J_a$  indicated in the leading  $LS$  term. Values in parentheses in the "BE" column represent binding of the anion state relative to the open- $s$  neutral threshold [3,4] with  $J=J_a-1/2$  and  $J=J_a+1/2$ , respectively. Unlike the  $7p$  attachments presented in Table II, this  $jj$  analysis, denoted by  $\langle j \rangle$ , is performed on the  $5f^m 6d^2$  or  $5f^q 6d^3$  portion of the neutral thresholds, representing the mixing of the corresponding anion total  $J$ 's when the  $7s$  attachment closes the  $7s^2$  subshell. Composition in both cases is presented rounded to the nearest percent.

Anion total $LS$ composition	BE	Neutral core $jj$ analysis
Th <sup>-</sup> $6d^3 7s^2$ ( $q=0$ )		Th $\langle 6d^3 \rangle 7s$
$^4F_{3/2}$ 86, $^2D$ 13, $^2P$ 1	304 (994, 1093)	$^5F_1: \langle 3/2 \rangle$ 100
$^4F_{5/2}$ 96, $^2D$ 4	164 (953, 1094)	$^5F_2: \langle 5/2 \rangle$ 50, $\langle 3/2 \rangle$ 50
$^4F_{7/2}$ 94, $^2G$ 6	28 (958, 1119)	$^5F_3: \langle 5/2 \rangle$ 71, $\langle 7/2 \rangle$ 29
		$^5F_4: \langle 7/2 \rangle$ 74, $\langle 9/2 \rangle$ 26
Pa <sup>-</sup> $5f^2 6d^2 7s^2$ ( $m=2$ )		Pa $\langle 5f^2 6d^2 \rangle 7s$
$^5L_6$ 84, $^3K$ 15, $^1I$ 1	134 (1002, 1189)	$^6L_{11/2}: \langle 6 \rangle$ 99, $\langle 5 \rangle$ 1
		$^6L_{13/2}: \langle 7 \rangle$ 52, $\langle 6 \rangle$ 48
Pa <sup>-</sup> $5f 6d^3 7s^2$ ( $q=1$ )		Pa $\langle 5f 6d^3 \rangle 7s$
$^5I_4$ 86, $^3H$ 12, $^1G$ 1, $^3G$ 1	52 (992, 1116)	$^6I_{7/2}: \langle 4 \rangle$ 99, $\langle 3 \rangle$ 1
		$^6I_{9/2}: \langle 5 \rangle$ 64, $\langle 4 \rangle$ 36
U <sup>-</sup> $5f^3 6d^2 7s^2$ ( $m=3$ )		U $\langle 5f^3 6d^2 \rangle 7s$
$^6M_{13/2}$ 84, $^4L$ 15, $^2K$ 1	260 (1035, 1267)	$^7M_6: \langle 13/2 \rangle$ 100
		$^7M_7: \langle 15/2 \rangle$ 64, $\langle 13/2 \rangle$ 36
Np <sup>-</sup> $5f^4 6d^2 7s^2$ ( $m=4$ )		Np $\langle 5f^4 6d^2 \rangle 7s$
$^7M_6$ 87, $^5L$ 12, $^3K$ 1	103 (985, 1213)	$^8M_{11/2}: \langle 6 \rangle$ 100
		$^8M_{13/2}: \langle 7 \rangle$ 57, $\langle 6 \rangle$ 43

tion effects and saturation of bases. Interestingly, the differences in these two Lr<sup>-</sup> values above are quite similar, particularly when the second case is shifted by the 18 meV difference in the  $^2D_{3/2}$  positions (155 vs 152 meV more binding in our RCI calculations). Later intermediate Hamiltonian coupled-cluster calculations gave an EA of 476 meV [6] in much better agreement with our  $5f^{14} 7s^2 7p^2 \ ^3P_0$  value, but the corresponding  $5f^{14} 6d 7s^2 7p$  state was predicted bound by 143 meV (smaller than the earlier 160 meV value [9]). Our  $^3F_2$  leading term of this odd state does agree with the later case, while the older work listed this state as  $^1D_2$ . The extra binding in our RCI calculations here that results in the third weakly bound  $^3P_1$  state of Table II is due to improved one-electron radial functions [1,2] and inclusion of extensive second-order effects.

Former RCI actinide EA studies of our own group in the mid-1990s were limited by the amount of correlation that could be included, since the codes at the time supported bases roughly one quarter to one third as large as the current version used in this study, and none of these universal  $jls$  restrictions on the  $5f$  electrons were possible. The simplest case, Th<sup>-</sup>, has been changed very little in this update with only 3 meV increase in the EA, 365 meV [23] vs 368 meV. In fact, the lowest levels of the other Th<sup>-</sup>  $J$ 's also agree with our earlier study to within 20 meV. Since this Th<sup>-</sup>  $q=0$  case was simple enough to include considerable second-order effects, the principle change in the  $7p$  attachments here is the

prediction of the additional weakly bound  $^2D_{3/2}$  and  $^2D_{5/2}$  excited states, which we attribute to improvements in the  $7p_{3/2}$  radial functions as described in the lanthanide work [1,2] (these states have only moderate  $7p_{3/2}$  mixing as shown in the "jj attachment" column of Table II, but the unbound third level of each of these two  $J$ 's has been lowered significantly). Increased binding of 115 and 108 meV of the  $7s$  attachments (as well as inclusion of the additional  $J=7/2$  state) is principally due to explicit inclusion of  $7p$  one-electron radial functions. For example, important  $7s^2 \rightarrow vp^2$  and  $6d 7s \rightarrow vp^2$  correlation was included using the screened hydrogenic "virtual" radial functions employed by our RCI methodology, but here we have additional  $6d^2$  and  $6d 7s$  correlation of  $6d^3 7p^2$  and  $6d^2 7s 7p^2$  (second-order quadruple replacements relative to  $6d^3 7s^2$ ) which was not present in the earlier work [23]. The more complicated cases of Pa<sup>-</sup> [24] and U<sup>-</sup> [25] could not accommodate as many second-order effects in the past, and the  $jls$   $5f^3$  restrictions have been particularly helpful in this study of U<sup>-</sup>. Our predictions here have increased the EA of Pa<sup>-</sup> by 162 meV and the EA of U<sup>-</sup> by 190 meV, the latter is larger due to even fewer second-order correlation than the former, e.g.,  $7s^2 \rightarrow sd+pf$  correlation was previously excluded from U<sup>-</sup> [25] but not from Pa<sup>-</sup> [24]. Similar increases in binding in the  $7s$  attachments have resulted in bound states as presented in Table III where none were predicted earlier, and our group had not considered attachments to the  $q=1$  thresholds of Pa prior to the present study.

On the experimental front, anion yields in accelerator mass spectrometry studies have indicated that the EA's of Th, Pa, U, and Pu are all  $>50$  meV [26,27]. The relative yields of  $\text{Th}^-:\text{Pa}^-:\text{U}^-$  in these experiments were 4:1:1 [26,27], and since this RCI study predicts similar EA's for these three anions (within a spread of 16 meV), we suggest the higher yield for  $\text{Th}^-$  may be due to the greater number of bound states, including the  $7s$  attachments of Table III. So far, laser photodetachment experiments have only been able to place upper bounds on actinide EA's based on incident photon energy, e.g.,  $\leq 1.165$  eV in the case of  $\text{Th}^-$  [28]. Hopefully, this comprehensive actinide survey will serve as encouragement to experimenters to reconsider actinide anion studies despite the difficulties of dealing with radioactive species.

## V. CONCLUSIONS

When presenting work pertaining an entire row of elements, it is perhaps expected but still regretful when some point is omitted in the deluge of data and details, and here we would like to make a few last comments regarding the prior lanthanide studies [1,2]. We should point out the reasonable agreement between our latest  $\text{Lu}^- 4f^{14}5d6s^26p$  BE's [2] and those of the recent calculations of Borschevsky *et al.* [6] cited in the  $\text{Lr}^-$  discussion above; an RCI EA of 353 meV vs their 336 meV (though our designations of  $^1D_2$  vs  $^3F_2$  disagree). These calculations predicted greater binding for the  $4f^{14}6s^26p^2$  state than our study, 167 [6] vs 78 meV, but our expectation is that the photodetachments from the  $4f^{14}5d6s^26p$  states are sufficient to explain the experimental spectrum of Davis and Thompson [29], so an experimental verification of either of these values may be difficult. Relativistic coupled-cluster calculations by Eliav *et al.* cited in the  $\text{Ac}^-$  discussion above predicted a  $^1D_2 6p$  attachment in  $\text{La}^-$  with an EA of 325 meV [22] compared to our RCI BE of 434 meV [2] for this state. However, the  $^3F_2$  and  $^3F_3 5d^26s^2$  levels of this  $\text{La}^-$  study [22] are over 350 meV less bound than our RCI predictions; our revised RCI calculations [2]

and the experimental analysis of Covington *et al.* [17] agree that this even  $^3F_2$  level is the  $\text{La}^-$  ground state. We pointed out the reasonable agreement of our  $\text{Tm}^-$  EA of 22 meV [1] with the 32 meV measurement of Nadeau *et al.* [27], but neglected to comment on the even better agreement of the splitting of the  $J=3$  and  $J=4$  levels, 8 vs 7 meV. Similarly, after much discussion of our newly predicted  $4f^25d^26s^2$  anion state in  $\text{Pr}^-$  and its possible explanation of the double peak seen in the experimental spectrum of Davis and Thompson [15], we neglected to point out that this state is of the same parity as the  $\text{Pr}^- 4f^36s^26p$  ground state and differs from its configuration by two electrons. The fact that its lifetime would likely be due to  $M1$  and  $E2$  decay (by a small amount of mixing of these  $n=3$  and  $m=2$  configurations that was not considered in these RCI studies) suggests that it would be a very long-lived state that would, in fact, be seen by the experiment [15].

The  $jls$ -restriction technique has been valuable not just because it allowed us to tackle mid-row lanthanides and actinides, but because of the ability to collect data and study trends throughout an entire row knowing that all the calculations were performed with similar levels of correlation. We have established a nearly linear trend in decrease of  $p$  attachment to  $f^ns^2$  states for both rows as in Fig. 2 with less binding and a slightly steeper slope in this actinide survey. Similarly, we have noted a consistency of  $s$  binding relative to neutral open- $s$  excited thresholds,  $\sim 860$  meV in the lanthanides [2] and  $\sim 990$  meV in this actinide study.

Future RCI work on these systems will perhaps require mixing of configurations with different  $f$  occupancies and calculations of photodetachment cross sections, both of which will likely require less strict trimming of the  $f^{n,m,q}$  bases. We are, however, encouraged by continued experimental [30] and computational [31] interest in these anions.

## ACKNOWLEDGMENTS

Support for this work from the National Science Foundation, Grant No. PHY-0652844, is gratefully acknowledged.

- 
- [1] S. M. O'Malley and D. R. Beck, Phys. Rev. A **78**, 012510 (2008).
- [2] S. M. O'Malley and D. R. Beck, Phys. Rev. A **79**, 012511 (2009).
- [3] *International Tables of Selected Constants*, edited by J. Blaise and J.-F. Wyart (Tables Internationales de Constantes, Paris, 1992), Vol. 20.
- [4] J. E. Sansonetti, W. C. Martin, and S. L. Young, *NIST Handbook of Basic Atomic Spectroscopic Data (version 1.1.2)* (National Institute of Standards and Technology, Gaithersburg, MD, 2009).
- [5] M. Sewtz, H. Backe, A. Dretzke, G. Kube, W. Lauth, P. Schwamb, K. Eberhardt, C. Grüning, P. Thörle, N. Trautmann, P. Kunz, J. Lassen, G. Passler, C. Z. Dong, S. Fritzsche, and R. G. Haire, Phys. Rev. Lett. **90**, 163002 (2003).
- [6] A. Borschevsky, E. Eliav, M. J. Vilkas, Y. Ishikawa, and U. Kaldor, Eur. Phys. J. D **45**, 115 (2007).
- [7] S. Fritzsche, C. Z. Dong, F. Koike, and A. Uvarov, Eur. Phys. J. D **45**, 107 (2007).
- [8] Y. Zou and C. F. Fischer, Phys. Rev. Lett. **88**, 183001 (2002).
- [9] E. Eliav, U. Kaldor, and Y. Ishikawa, Phys. Rev. A **52**, 291 (1995).
- [10] S. Fritzsche, Eur. Phys. J. D **33**, 15 (2005).
- [11] A. Borschevsky, E. Eliav, M. J. Vilkas, Y. Ishikawa, and U. Kaldor, Phys. Rev. A **75**, 042514 (2007).
- [12] S. M. O'Malley and D. R. Beck, Phys. Rev. A **77**, 012505 (2008).
- [13] *Atomic Energy Levels—The Rare-Earth Elements*, edited by W. C. Martin, R. Zalubas, and L. Hagan, (U.S. GPO, Washington, D.C., 1978).
- [14] Yu. Ralchenko, A. E. Kramida, J. Reader, and NIST ASD Team, *NIST Atomic Spectra Database (version 3.1.5)* (National

- Institute of Standards and Technology, Gaithersburg, MD, 2009).
- [15] V. T. Davis and J. S. Thompson, *J. Phys. B* **35**, L11 (2002).
- [16] S. H. Vosko, J. B. Lagowski, I. L. Mayer, and J. A. Chevary, *Phys. Rev. A* **43**, 6389 (1991).
- [17] A. M. Covington, D. Calabrese, J. S. Thompson, and T. J. Kvale, *J. Phys. B* **31**, L855 (1998).
- [18] V. T. Davis and J. S. Thompson, *Phys. Rev. Lett.* **88**, 073003 (2002).
- [19] X. Cao and M. Dolg, *Phys. Rev. A* **69**, 042508 (2004).
- [20] C. W. Walter, N. D. Gibson, C. M. Janczak, K. A. Starr, A. P. Snedden, R. L. Field III, and P. Andersson, *Phys. Rev. A* **76**, 052702 (2007).
- [21] Y. Guo and M. A. Whitehead, *Phys. Rev. A* **40**, 28 (1989).
- [22] E. Eliav, S. Shmulyian, U. Kaldor, and Y. Ishikawa, *J. Chem. Phys.* **109**, 3954 (1998).
- [23] D. Datta and D. R. Beck, *Phys. Rev. A* **50**, 1107 (1994).
- [24] K. D. Dinov and D. R. Beck, *Phys. Rev. A* **53**, 4031 (1996).
- [25] K. D. Dinov and D. R. Beck, *Phys. Rev. A* **52**, 2632 (1995).
- [26] X.-L. Zhao, M.-J. Nadeau, M. A. Garwan, L. R. Kilius, and A. E. Litherland, *Phys. Rev. A* **48**, 3980 (1993).
- [27] M.-J. Nadeau, M. A. Garwan, X.-L. Zhao, and A. E. Litherland, *Nucl. Instrum. Methods Phys. Res. B* **123**, 521 (1997).
- [28] D. Berkovits, E. Boaretto, M. Paul, and G. Hollos, *Rev. Sci. Instrum.* **63**, 2825 (1992).
- [29] V. T. Davis and J. S. Thompson, *J. Phys. B* **34**, L433 (2001).
- [30] K. C. Chartkunchand, V. T. Davis, S. S. Duvvuri, Z. A. McCormick, J. S. Thompson, P. P. Wiewior, and A. Covington, *Bull. Am. Phys. Soc.* **54**, No. 7, 172 (2009), <http://meetings.aps.org/link/BAPS.2009.DAMOP.Y1.45>
- [31] Z. Felfli, A. Z. Msezane, and D. Sokolovski, *Phys. Rev. A* **79**, 012714 (2009).